

Jet Observables of Parton Energy Loss in High-Energy Nuclear Collisions

Ben-Wei Zhang^{a,b}

^a*Los Alamos National Laboratory, Theoretical Division, MS B238, Los Alamos, NM 87545, USA*

^b*Key Laboratory of Quark & Lepton Physics (Hua-Zhong Normal University), Ministry of Education, China*

Abstract

While strong attenuation of single particle production and particle correlations has provided convincing evidence for large parton energy loss in the QGP, its application to jet tomography has inherent limitations due to the inclusive nature of the measurements. Generalization of this suppression to full jet observables leads to an unbiased, more differential and thus powerful approach to determining the characteristics of the hot QCD medium created in high-energy nuclear collisions. In this article we report on recent theoretical progress in calculating jet shapes and the related jet cross sections in the presence of QGP-induced parton energy loss. (i) A theoretical model of intra-jet energy flow in heavy-ion collisions is discussed. (ii) Realistic numerical simulations demonstrate the nuclear modification factor $R_{AA}(p_T)$ evolves continuously with the jet cone size R^{\max} or the acceptance cut ω_{\min} - a novel feature of jet quenching. The anticipated broadening of jets is subtle and most readily manifested in the periphery of the cone for smaller cone radii.

1. Introduction

When a fast quark or gluon traverses a hot/dense nuclear medium, it may undergo multiple scattering with other partons in the medium and lose a large amount of its energy via induced gluon bremsstrahlung [1]. This jet quenching mechanism has been used to successfully explain the strong suppression of the hadron spectra at large transverse momentum observed in nucleus-nucleus collisions at the Relativistic Heavy Ion Collider (RHIC). However, at present, most measurements of hard processes are limited to inclusive hadron (or photon) production and di-hadron (or gamma-hadron) correlations, which are only the leading fragments of a jet. Thus their measurement may suffer from geometric biases [2]. With the upgrades at the RHIC experimental facilities and the new opportunities provided by LHC, much more differential studies of parton energy loss in nuclei will become available - the ability to investigate the full structures of a jet in relativistic heavy-ion collisions [3, 4]. In this article we review our recent theoretical progress on calculating jet shapes and the related jet cross sections in reactions with ultra-relativistic nuclei [5], which become feasible as a new, differential and accurate test of the underlying QCD theory. Our theoretical approach to understanding the jet shapes in the vacuum as well as the medium-induced jet shapes with experimental acceptance cut will be discussed. We will also show numerical simulations and their implications for the current heavy-ion program.

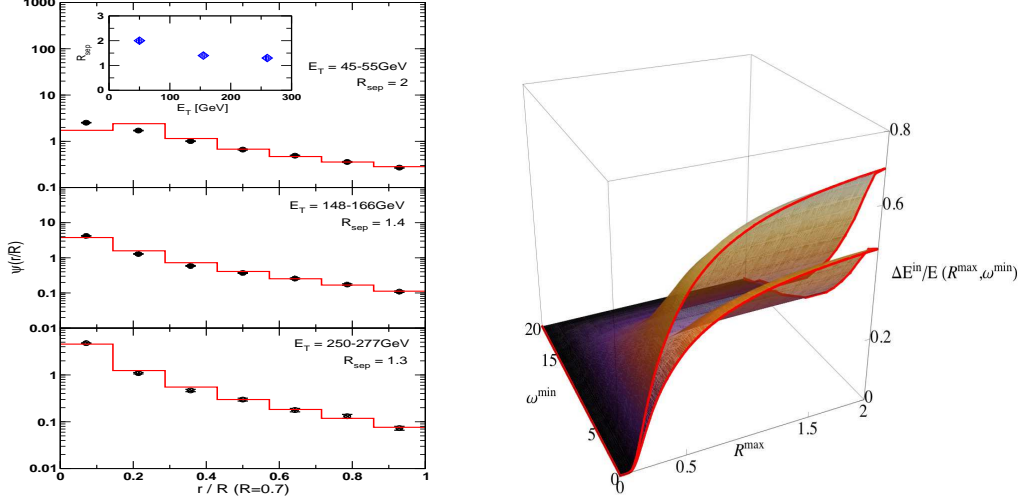


Figure 1: (Left panel) Comparison of numerical results from our theoretical calculation to experimental data on differential jet shapes at $\sqrt{s} = 1960$ GeV by CDF II [7]. (Right panel) 3D plot for the ratio of the energy that a partons loses inside a jet cone of opening angle R^{\max} with $\omega > \omega^{\min}$ to the total parton energy with $E_{\text{jet}} = 20$ GeV in $b = 3$ fm Pb+Pb collisions at LHC.

2. Jet shapes in p+p collisions

The jet shape, related to the intra-jet energy flow, is one of the most common ways of resolving the internal jet structure. The usual definition of an “integral jet shape” reads [6]:

$$\Psi_{\text{int}}(r; R) = \frac{\sum_i (E_T)_i \Theta(r - R_{i,\text{jet}})}{\sum_i (E_T)_i \Theta(R - R_{i,\text{jet}})}. \quad (1)$$

Here r, R are Lorentz-invariant opening angles, $R_{i,\text{jet}} = \sqrt{(\eta_i - \eta_{\text{jet}})^2 + (\phi_i - \phi_{\text{jet}})^2}$ in a cone algorithm, and i represents a sum over all particles in this jet. With the above definition we have $\Psi_{\text{int}}(R; R) = 1$. A differential jet shape is defined as follows:

$$\psi(r; R) = \frac{d\Psi_{\text{int}}(r; R)}{dr}, \quad (2)$$

and $\psi(r; R)dr$ gives the fraction of all energy within a cone with the size R around the jet axis that is within an annulus of radius r and width dr , centred on the jet axis.

We follow an analytical approach by Seymour [6], generalize it to include finite experimental acceptance cut effect, and find [5]:

$$\psi(r) = \psi_{\text{coll}}(r)(P(r) - 1) + \psi_{\text{LO}}(r) + \psi_{i,\text{LO}}(r) + \psi_{\text{PC}}(r) + \psi_{i,\text{PC}}(r). \quad (3)$$

On the right-hand-side of Eq. (3) the first term represents the contribution from Sudakov resummation with subtraction to avoid double counting; the second and third terms give the leading-order contributions in the final-state and the initial-state splitting, respectively; the last two terms come from power corrections when integrating over the Landau pole. In the left panel of Fig. 1 we show the comparison of our theoretical results for jet shapes to the CDF II data. It can be

seen that the pQCD calculation yields a good description of the jet shapes measured at the CDF, and thus provides a reliable baseline in $p + p$ collisions for comparison to the full in-medium jet shape in heavy-energy nuclear reactions.

3. Energy distribution due to medium-induced gluon radiation

When an energetic parton propagates inside the QGP, it will lose energy via induced gluon radiation. This will give rise to additional contributions to jet shapes. In this study, we adopt the GLV formalism to calculate the in-medium jet shapes [8, 9]. An important feature of the induced final-state bremsstrahlung in the deep LPM regime is that there is no collinear divergence [9] and, thus, no resummation is needed when $r \rightarrow 0$. In the GLV formalism, the intensity spectrum due to final-state gluon radiation can be written as [5]:

$$k^+ \frac{dN^g(FS)}{dk^+ d^2\mathbf{k}} = \frac{C_R \alpha_s}{\pi^2} \sum_{n=1}^{\infty} \left[\prod_{i=1}^n \int \frac{d\Delta z_i}{\lambda_g(z_i)} \right] \left[\prod_{j=1}^n \int d^2\mathbf{q}_j \left(\frac{1}{\sigma_{el}(z_j)} \frac{d\sigma_{el}(z_j)}{d^2\mathbf{q}_j} - \delta^2(\mathbf{q}_j) \right) \right] \\ \times \left[-2 \mathbf{C}_{(1, \dots, n)} \cdot \sum_{m=1}^n \mathbf{B}_{(m+1, \dots, n)(m, \dots, n)} \left(\cos \left(\sum_{k=2}^m \omega_{(k, \dots, n)} \Delta z_k \right) - \cos \left(\sum_{k=1}^m \omega_{(k, \dots, n)} \Delta z_k \right) \right) \right].$$

With growing jet cone radius R_{\max} more of the lost energy, carried away by radiated gluons, will fall back again inside the cone; conversely with larger acceptance cut ω^{\min} , a larger energy fraction will not be measured. The right panel of Fig. 1 illustrates our numerical results for the fractional energy loss inside the jet cone as a function of the cone size R_{\max} and the experimental acceptance cut ω^{\min} , defined as:

$$\frac{\Delta E^{in}}{E}(R^{\max}, \omega^{\min}) = \frac{1}{E} \int_{\omega^{\min}}^E d\omega \int_0^{R^{\max}} dr \frac{dI^g}{d\omega dr}(\omega, r). \quad (4)$$

4. Jet tomography in high-energy nuclear collisions

Taking into account the contributions to the jet shape from vacuum splitting and the medium-induced bremsstrahlung, we can obtain the full jet shape in high-energy nuclear collisions as:

$$\psi_{\text{tot.}}(r/R) = \frac{1}{\text{Norm}} \int_{\epsilon=0}^1 d\epsilon \sum_{q,g} P_{q,g}(\epsilon) \frac{1}{(1 - (1 - f_{q,g}) \cdot \epsilon)^3} \\ \times \frac{\sigma_{q,g}^{NN}(R, \omega^{\min})}{d^2 E_T' dy} \left[(1 - \epsilon) \psi_{\text{vac.}}^{q,g}(r/R) + f_{q,g} \cdot \epsilon \psi_{\text{med.}}^{q,g}(r/R) \right]. \quad (5)$$

In Eq. (5) $f = \Delta E_{\text{rad}} \{(0, R); (\omega^{\min}, E)\} / \Delta E_{\text{rad}} \{(0, R^{\infty}); (0, E)\}$ gives the fraction of the lost energy that falls within the jet cone, $r < R$, and carried by gluons of $\omega > \omega^{\min}$ relative to the total parton energy loss without the above kinematic constraints. Furthermore, ϵ is the total fractional energy loss and $P(\epsilon)$ represents the related probability distribution.

We can also calculate the related jet cross section with parton energy loss in $A + A$ collisions [5] and generalize the nuclear modification factor of leading hadrons to that of jets as follows:

$$R_{AA}^{\text{jet}}(E_T; R^{\max}, \omega^{\min}) = \frac{\frac{d\sigma^{AA}(E_T; R^{\max}, \omega^{\min})}{dy d^2 E_T}}{\langle N_{\text{bin}} \rangle \frac{d\sigma^{pp}(E_T; R^{\max}, \omega^{\min})}{dy d^2 E_T}}. \quad (6)$$

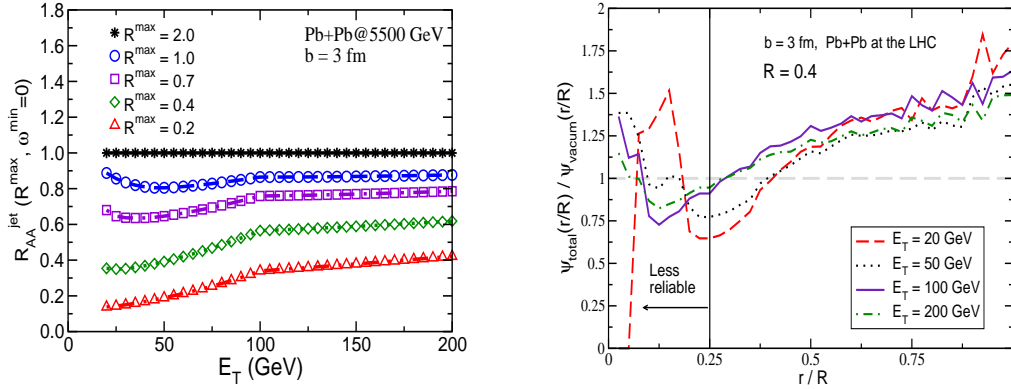


Figure 2: (Left panel) Nuclear modification factor $R_{AA}^{\text{jet}}(R^{\text{max}}, \omega^{\text{min}})$ as a function of E_T for different jet cone radii R^{max} . (Right panel) The ratios of the total jet shape in high-energy nuclear collisions to the jet shape in vacuum with cone radius $R = 0.4$. Results are for Pb+Pb collision at $\sqrt{s} = 5.5$ TeV with $b = 3$ fm.

Based on the analytic pQCD model we are now ready to perform numerical simulations and several selected results are shown in Fig. 2. We see that with altering cone radius $R_{AA}^{\text{jet}}(E_T; R^{\text{max}}, \omega^{\text{min}})$ changes continuously and reaches unity for large radii ($R^{\text{max}} = 2.0$) when all of the lost energy falls back inside the cone. This is in stark contrast to a single R_{AA} curve for inclusive hadron production observed at RHIC. Therefore, measurements of the suppression of jet cross sections for different R^{max} will provide an independent and much more accurate way to determine the characteristics of parton energy loss in the QGP. The right panel of Fig. 2 illustrates that the QGP broadening effects are manifest in the tails of the energy flow distribution and the enhancement factor due to medium-induced jet shapes can be about 1.75 when $r/R \sim 1$ with $R = 0.4$.

Acknowledgments

We thank I. Vitev, S. Wicks, M. H. Seymour, H. Caines, N. Grau, H. Takai, S. Salur and M. Ploskon for many helpful discussions. This research is supported by the US Department of Energy, Office of Science, under Contract No. DE-AC52-06NA25396 and in part by the LDRD program at LANL, the MOE of China under Project No. IRT0624 and the NNSF of China.

References

- [1] M. Gyulassy, I. Vitev, X. N. Wang and B. W. Zhang, arXiv:nucl-th/0302077.
- [2] S. Salur [for the STAR Collaboration], arXiv:0907.4536 [nucl-ex].
- [3] M. Ploskon [for the STAR Collaboration], arXiv:0908.1799 [nucl-ex].
- [4] N. Grau [for the ATLAS collaboration], arXiv:0907.4944 [nucl-ex].
- [5] I. Vitev, S. Wicks and B. W. Zhang, JHEP **0811** (2008) 093 [arXiv:0810.2807 [hep-ph]]; I. Vitev, B. W. Zhang and S. Wicks, Eur. Phys. J. C **62**, 139 (2009) [arXiv:0810.3052 [hep-ph]].
- [6] M. H. Seymour, Nucl. Phys. B **513**, 269 (1998);
- [7] D. E. Acosta *et al.* [CDF Collaboration], Phys. Rev. D **71**, 112002 (2005) [arXiv:hep-ex/0505013].
- [8] M. Gyulassy, P. Levai and I. Vitev, Phys. Rev. Lett. **85**, 5535 (2000); I. Vitev, Phys. Rev. C **75**, 064906 (2007).
- [9] I. Vitev and B. W. Zhang, Phys. Lett. B **669** (2008) 337; I. Vitev, Phys. Lett. B **630**, 78 (2005).